

Figure 4. In-phase (χ') and out-of-phase (χ'') components of the ac magnetic susceptibility plotted as a function of temperature at the frequencies indicated for $\text{Fe}_5(\text{InTe}_4)_2$.

periment at lower temperatures, whereas the IRM is little affected by the temperature. This is shown in Figure 3 where both TRM and IRM at an applied field of 3 kG are plotted as a function of temperature. The TRM and IRM curves merge near 15 K, the freezing point, which agrees with the susceptibility data at zero field cooling and field cooling.

There are some pronounced differences between the dc and ac magnetic susceptibility data. The in-phase magnetic susceptibility (χ') and the out-of-phase magnetic susceptibility (χ'') are plotted together in Figure 4. The in-phase magnetic ac susceptibility (χ') exhibits a broad maximum with two humps, one at approximately 32 K and the other near 15 K. The out-of-phase component (χ'')

vanishes above 40 K, but at low temperatures two maxima in accordance with the behavior of χ' are seen. The sharper peak in χ'' occurs at lower temperatures (ca. 15 K) and corresponds to the anomaly observed in the dc magnetic measurements. The change in the frequency of the ac experiment causes the anomalies to shift to slightly higher temperatures at higher frequencies. This effect is more pronounced at the anomaly around 15 K than at the anomaly at higher temperature. The higher temperature hump in the ac magnetic susceptibility data likely arises from short-range ferromagnetic ordering in accordance with the prediction from the high-temperature Curie-Weiss fits.

The behavior of the χ' and χ'' data point to $\text{Fe}_5(\text{InTe}_4)_2$ being an amorphous ferromagnetic material that begins to undergo extended short-range order around 35 K. This is consistent with the high-temperature Curie-Weiss fit of the dc magnetic data. At lower temperatures, a blocking of the domain wall migration sets in but is overruled by the spin-glass-like anomalies around 15 K. It is important to emphasize the dc data were measured in an applied magnetic field, while the ac data were measured at near zero field conditions. This could account for some of the apparent discrepancy between the ac and dc magnetic susceptibility data. A more detailed analysis of the present class of magnetic materials with special attention to the behavior of the magnetization as a function of field in the temperature region between 15 and 30 K will be reported in the near future.

Acknowledgment. C.J.O. acknowledges support from a grant from the Louisiana Education Quality Support Fund administered by the Board of Regents of the state of Louisiana and the donors of the Petroleum Research Fund, administered by the American Chemical Society.

Decomposition of Trimethylaluminum on Si(100)

T. R. Gow, R. Lin, L. A. Cadwell, F. Lee, A. L. Backman, and R. I. Masel*

Department of Chemical Engineering, University of Illinois, 1209 W. California St., Urbana, Illinois 61801

Received January 9, 1989

The mechanism of trimethylaluminum (TMAI) decomposition on a heated Si(100) substrate is studied by using temperature-programmed desorption, X-ray photoelectron spectroscopy, and electron energy loss spectroscopy. It is found that the TMAI adsorbs as dimers at low temperature. The dimers dissociate into monomers upon heating to 300–400 K. Further heating causes one of the methyl groups in the TMAI to react with a hydrogen on another methyl group, liberating methane. This leaves a CH_2 group bound to the aluminum, which is seen clearly with EELS. Upon further heating, some of the remaining fragments undergo another intramolecular hydrogen shift, producing additional methane. The other fragments dissociate into aluminum atoms and CH_x groups. The CH_x groups are strongly bound on silicon. Hence, they decompose above 750 K, yielding adsorbed hydrogen and adsorbed carbon. The hydrogen desorbs between 750 and 850 K. The carbon remains bound to the silicon to high temperatures. These results show that carbon incorporation is an intrinsic part of the TMAI decomposition process on Si(100). Thus, TMAI would not be an appropriate source gas when one needs to produce films with very low carbon levels.

Introduction

This paper is a continuation of previous work on the surface chemistry of molecules of interest for MOCVD and MOMBE.^{1,2} The paper will focus on the mechanism of trimethylaluminum (TMAI) decomposition at low pressures on Si(100). Trimethylaluminum is an important

source gas for the growth of aluminum films on various substrates. It is also used as a source gas in $\text{Al}_x\text{Ga}_{1-x}\text{As}$ growth by MOCVD. However, aluminum films grown with TMAI show high carbon levels and a columnar morphology. $\text{Al}_x\text{Ga}_{1-x}\text{As}$ films grown with TMAI often have high

(1) Lee, F.; Gow, T. R.; Masel, R. I. *J. Electrochem. Soc.*, in press.
(2) Lee, F.; Backman, A.; Lin, R.; Gow, T. R.; Masel, R. I. *Surf. Sci.*, in press.

* To whom correspondence should be sent.

carbon levels. Thus, while TMAI is a common source gas, it is not ideal for many applications.

At present, it is not known why the carbon incorporation or the columnar morphology occurs. Part of the problem is that the chemistry of TMAI decomposition on semiconductor substrates is largely unknown. In a previous study, Squire, et al.³ directed a beam of TMAI at a variety of heated substrates and used mass spectroscopy to look for desorption products. Squire et al. were not able to detect any desorption products during their initial exposure of TMA. However, after they built up a "metallic aluminum" layer over the substrate, they observed the desorption of methyl radicals above 650 K using resonance multiphoton ionization. Nevertheless, they were not able to detect any desorption products below 600 K. Further, no methane desorption was detected under any conditions by using electron impact (EI) ionization. Of course, the main mass fraction of methane (16 amu) is also one of the EI cracking fractions of TMAI. Thus, it is unclear whether Squire et al. could have observed the production of a small amount of methane in their experiments. However, Squire et al. argued that it was significant that they were able to observe methyl radicals but not methane. As a result, Squire et al. proposed that the main pathway for TMAI decomposition was direct desorption of methyl radicals.

In the work reported here, we have examined TMAI decomposition on Si(100) using a variety of surface spectroscopic techniques in an attempt to see if there is a mechanism for TMAI decomposition in addition to the one observed by Squire et al. Aluminum deposition on silicon is important technologically. It is thought that the initial stages of growth on the silicon substrate control the morphology of the resultant film. Thus, a study of the decomposition of TMAI on a silicon surface looked quite interesting.

At the same time one should recognize that we are not studying film growth directly. The chemistry occurring on a silicon substrate may well be different than the chemistry that occurs during the steady-state growth of aluminum or aluminum gallium arsenide films. In particular, previous work has shown that the bond energy of a CH_x group is larger on a silicon atom than on an aluminum, gallium, or arsenic atom.¹⁵ Thus, one needs to be careful about extrapolating the results here to film-growth conditions. Still, the results here are directly applicable to the initial stages of aluminum growth on silicon substrates. Further, they may give some insights into the processes that occur in steady-state film growth.

Experimental Section

The experiments here were done using standard surface science techniques. A 1 cm \times 1.5 cm rectangular sample was cut from 0.05 or 8 Ω cm Si(100) wafers. The samples were rinsed with HF, mounted on tantalum clips, and then placed in one of three ultra-high-vacuum systems. Each vacuum system had a fairly standard design. One of the vacuum systems was equipped with a LK 2000-DAC HREELS spectrometer, while a second vacuum system was equipped with a PHI 545 XPS unit. The third vacuum system was equipped with a shielded Balzers QMG 112a mass spectrometer for TPD. All three vacuum systems were also equipped with many of the standard surface science tools, including an AES unit, argon ion sputtering, a calibrated dosing system, and a mass spectrometer. The base pressures in the various systems were between 2×10^{-10} and 5×10^{-11} Torr.

Trimethylaluminum (TMAI) used for the work here was purchased from CVD Inc. The TMAI was freeze-thaw degassed and then admitted into the chamber through a calibrated quartz

capillary doser. The dosing system was passivated for several hours and turbopumped to minimize TMAI decomposition. Nevertheless, we are not sure whether some of the TMAI decomposed in the dosing tube. Thus, we can only report nominal TMAI exposures in the figures below, where the nominal exposure is defined as the exposure that the sample would have received if none of the TMAI had decomposed in the dosing tube.

The same general procedure was used in all the experiments reported here. The sample was cleaned until no impurities could be detected by AES. The sample was then exposed to a measured nominal dose of TMAI. The sample was heated, and TPD, XPS, and EELS were used to examine how the TMAI reacted as it was heated.

During an XPS run, the sample was sputtered and annealed until no impurities could be detected by XPS. The sample was then cooled to 300 K. Purified TMAI was dosed onto the sample through a dosing tube. The arrangement was such that only the front face of the sample was exposed to TMAI. The sample was then aligned with the XPS spectrometer, and a spectrum was recorded. Subsequent spectra were taken by annealing the sample to various temperatures, cooling back to 300 K, and then recording another spectrum.

The EELS data were taken by using procedures similar to those for XPS. The sample was cleaned until no impurities could be detected by AES and then a "clean" EELS spectrum was recorded. Next, the sample was dosed with TMAI through the calibrated leak system. The dosing was done at 120 K for those runs below 300 K and at 300 K for the runs at 300 K or more. The sample was then aligned with the EELS spectrometer, and a spectrum was recorded. Subsequent spectra were taken by sequentially annealing the sample to various temperatures, cooling to 120 or 300 K, and then recording another spectrum. Some runs were also done where the layer was reprepared between annealing steps. However, the results of those runs were essentially identical with those taken by using sequential heating. There was some buildup of water after several hours at 120 K. Hence, care was taken to periodically reprepare the TMA layer when we were running at 120 K.

There is one other detail of note. Even though the sample looked clean by AES, it was always possible to detect a surface carbon peak at $\sim 800 \text{ cm}^{-1}$ in EELS corresponding to $(0.5\text{--}3) \times 10^{13}$ atoms/ cm^2 of carbon. This peak could not be completely eliminated by any cleaning procedure.

The TPD spectra were taken as described previously.¹ The sample was cleaned as described above. The front of the sample was then exposed to a measured amount of TMAI. The sample was rotated in front of the mass spectrometer. The geometry was such that only molecules desorbing from the front of the sample could be detected. Then the sample was heated resistively at a constant rate of 10 K/s, and a TPD spectrum was recorded. Temperatures were measured with a chromel-alumel thermocouple bonded to the sample. All of the other procedures were standard. One is referred to our previously published work for more details.^{1,2}

Results

Figures 1–3 show a series of TPD spectra taken by exposing a clean Si(100) sample to between 2×10^{14} and 2×10^{15} molecules/ cm^2 of TMAI and then heating at 10 K/s. At low TMAI exposures, one observes a single hydrogen peak at 780 K shown in Figure 1. The hydrogen peak grows with increasing exposure. Simultaneously, one observes a series of molecular TMAI features extending up to 550 K in Figure 3. There is also a broad 16 amu peak in the spectrum between 350 and 750 K in Figure 2. The 16 amu peak can be decomposed into contributions from methane desorption and cracking of desorbing molecular TMAI in the mass spectrometer as shown in Figure 4.

We have also looked for other species including methyl radicals and C_2 hydrocarbons. No C_2H_x fragments were detected with a clean silicon substrate. However, there may be some desorption of C_2 fragments when the surface was contaminated with aluminum. Methyl radicals are difficult to detect with our experimental setup since the

(3) Squire, D. W.; Dulcey, C. S.; Lin, M. C. *J. Vac. Sci. Technol., B* 1985, 3, 1513.

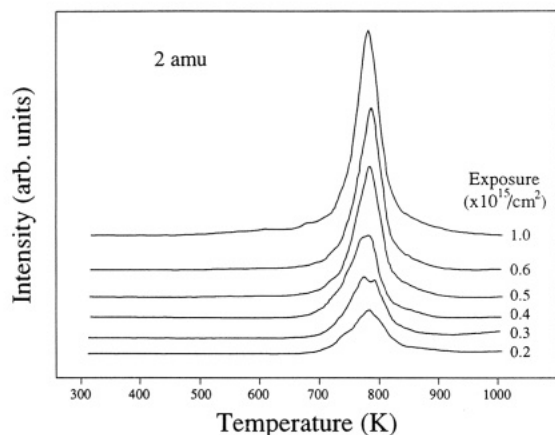


Figure 1. Series of 2 amu TPD spectra taken by exposing a 300 K Si(100) sample to various amounts of TMAI and then heating at 10 K/s. The exposures in the figure are nominal exposures; see text.

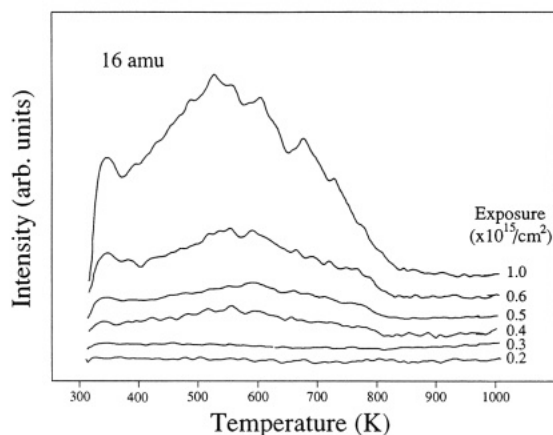


Figure 2. Series of 16 amu TPD spectra taken by exposing a 300 K Si(100) sample to various amounts of TMAI and then heating at 10 K/s. The exposures in the figure are nominal exposures; see text.

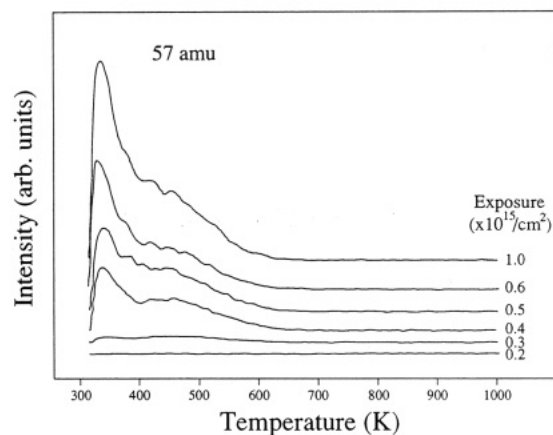


Figure 3. Series of 57 amu TPD spectra taken by exposing a 300 K Si(100) sample to various amounts of TMAI and then heating at 10 K/s. The exposures in the figure are nominal exposures; see text.

main cracking fraction of methyl radicals (15 amu) is also one of the main cracking fractions of methane. However, when we took our 15 amu spectrum and subtracted the expected cracking fraction of methane, we did find a small residual peak at 600 K. This suggests that there may be a minor decomposition pathway involving methyl radical desorption. However, methyl radical desorption is never a major pathway under our conditions.

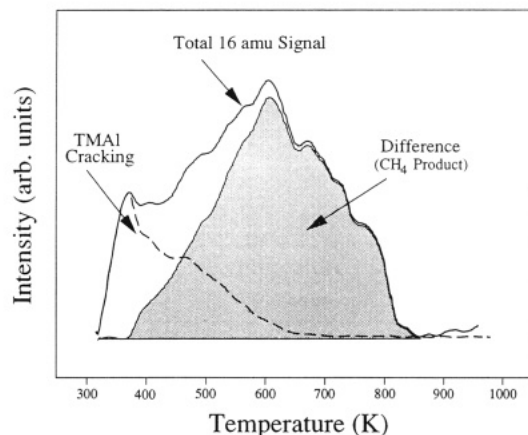


Figure 4. Deconvolution of the 5×10^{14} molecules/cm² 16 amu spectrum into contributions from TMAI cracking and methane: solid line, total mass 16; dashed line, contribution from TMAI cracking; shaded curve, difference.

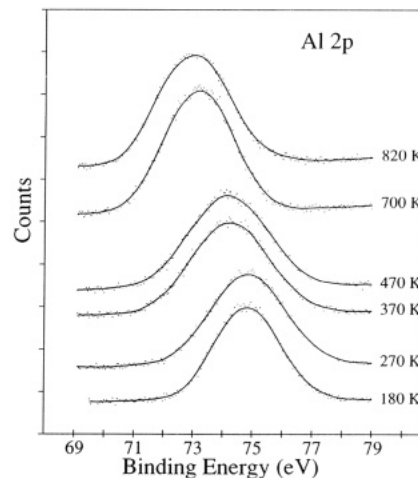


Figure 5. Series of Al_{2p} XPS spectra taken by exposing a 180 K Si(100) sample to a nominal 20-langmuir exposure of TMAI and then annealing as indicated.

Figure 5 shows a series of Al_{2p} XPS spectra taken by exposing a clean Si(100) sample to 2×10^{16} molecules/cm² of TMAI and then annealing as indicated. At low temperatures, a Al_{2p} peak is seen at 74.7 eV independent of coverage. The peak is slightly attenuated upon heating to 270 K. However, little change is seen in the peak position. Heating to 370 K produces a broadening of the Al_{2p} peak and a shift in the peak position to 74.1 eV. Heating to 470 K produces little additional change in the peak. Further heating to about 700 K produces a sharpening of the peak and a shift to 72.9 eV. The peak is then stable to 900 K. In other experiments we found that the XPS spectrum of aluminum evaporated on silicon also shows an Al_{2p} peak at 72.9 eV. Integration of the peak area indicates that the number of aluminum atoms is nearly constant between 270 and 800 K.

Figure 6 shows a series of C_{1s} spectra taken under the same conditions as those used to take the data in Figure 5. At 180 K, one observes a single C_{1s} peak at 285.2 eV, independent of exposure. The peak position is constant upon heating to 270 K, while the peak intensity decreases slightly. Further heating produces a continual shift in the C_{1s} peak to 282.5 eV. Chemisorbed carbon also shows a C_{1s} XPS peak at 282.5 eV. Integration of the peak areas indicates that at saturation, about 42% of the carbon in the TMAI remains behind on the surface.

Figure 7 shows a series of EELS spectra taken by condensing many layers of TMAI onto the surface and heating

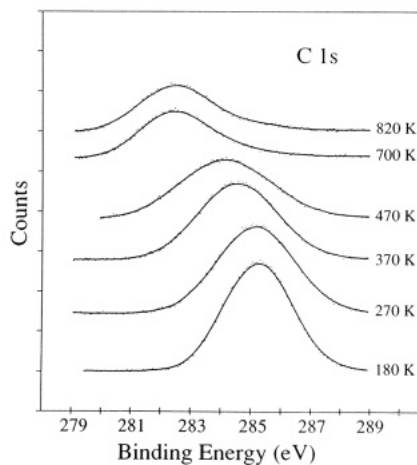


Figure 6. Series of C_{1s} XPS spectra taken by exposing a 180 K Si(100) sample to a nominal 20-langmuir exposure of TMAI and then annealing as indicated.

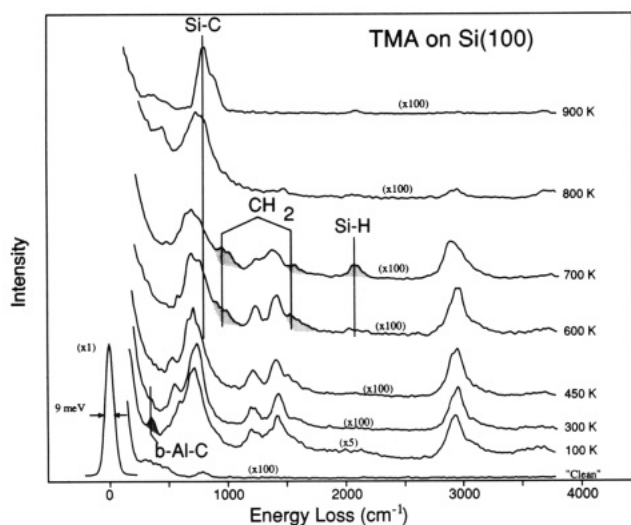


Figure 7. Series of EELS spectra taken by exposing a clean Si(100) sample to nominally 1×10^{16} molecules/cm² of TMAI at 100 K and then annealing as indicated.

as indicated. At 100 K, there are multilayers on the surface. The EELS spectrum shows broad peaks at 346, 590, 720, 1227, 1422, and 2933 cm^{-1} . Heating to 300 K produced a marked decrease in the absolute peak intensities. The 346- cm^{-1} peak has almost disappeared, while the peak at about 590 cm^{-1} has become more distinct. Nevertheless, there is little change in the positions of the various peaks. Heating to 450 K produces very little change in the main peaks in the spectra. However, there is some evidence for new shoulders at about 900 and 1520 cm^{-1} . The shoulders at 900 and 1520 cm^{-1} grow upon heating to 600 K. Further, new peaks appear at about 800 and 2070 cm^{-1} . The peaks at 800 and 2070 cm^{-1} grow upon heating to 700 K, while the 720-, 1227-, and 1420- cm^{-1} peaks shrink. Simultaneously, the shoulders at 900 and 1500 cm^{-1} become more distinct. Most of the peaks disappear upon heating to 800 K. However, a broad peak at about 800 cm^{-1} remains. The broad peak converts to a doublet at 800 and 870 cm^{-1} upon heating to 900 K.

Discussion

It is useful to discuss the work here in terms of the mechanism shown in Figure 8. The data in Figures 5-7 indicate that at 100 K the adsorption of TMAI is molecular. The peak positions in the XPS and EELS spectra are independent of whether there is a single layer or many

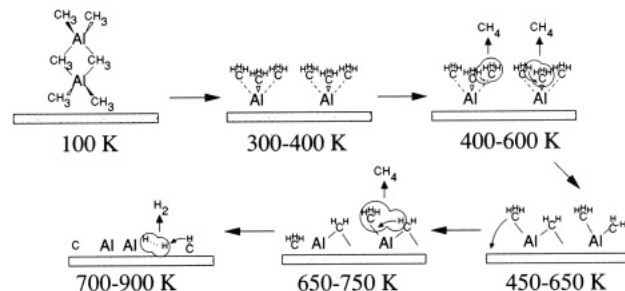


Figure 8. Proposed mechanism for TMAI decomposition on Si(100). Monomeric TMAI is actually a planar molecule,¹⁴ and we believe that it retains its planar configuration on the surface. However, we have distorted the TMAI in the diagram to simplify the picture.

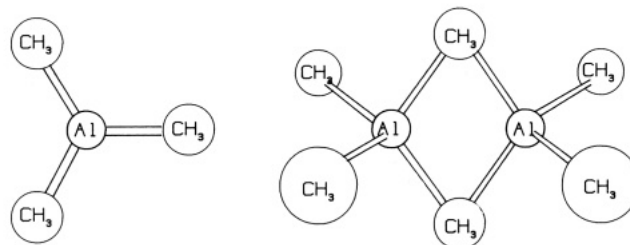


Figure 9. Structure of TMAI monomers and dimers from ref 14.

Table I. Comparison of the Modes (cm^{-1}) of Molecular TMAI Observed Here to Kvisle and Rytter's Spectra⁴ for Matrix-Isolated TMAI

mode	ref 4		TMAI on Si(100) (100 K)
	TMAI dimers	TMAI monomers	
bridged Al-C str	370		350
terminal Al-C str	563		540
Al-C ₃ str		689	
terminal CH ₃ rock	725	742	720
bridged CH ₃ rock	768		
CH ₃ sym def	1208	1196	1210
CH ₃ asym def	1435	1430	1430
CH ₃ asym str (A_2'')	2936	2948	2930
CH ₃ asym str (E')		2971	

layers of TMAI on the surface. Further, the measured peak positions in EELS compare very well to those of Kvisle and Rytter⁶ for solid TMAI, as shown in Table I. Thus, it seems that the adsorption of TMAI is molecular at 100 K.

The EELS data also show that the TMAI forms dimers at 100 K. Previous work has shown that TMAI forms dimers in the gas phase below 400 K. Figure 9 shows a diagram of the dimers. Notice that there are two kinds of CH₃ groups in the dimers, bridge bound CH₃ groups and terminal CH₃ groups. Kvisle and Rytter have shown that the bridged bound CH₃ groups have a characteristic Al-C stretching mode at 370 cm^{-1} . A mode at 350 cm^{-1} is clearly seen in the 100 K spectrum in Figure 7. Thus it appears that the TMAI adsorbs as dimers on Si(100) at low temperatures as suggested previously by Motooka et al.^{7,8}

(4) Squire, D. W.; Dulcey, C. S.; Lin, M. C. *Proc. Mater. Res. Soc.* **1986**, *54*, 709.

(5) Squire, D. W.; Dulcey, C. S.; Lin, M. C. *Chem. Phys. Lett.* **1986**, *131*, 112.

(6) Kvisle, S.; Rytter, E. *Spectrochim. Acta* **1984**, *40*, 939.

(7) Salaneck, W. R.; Bergman, R.; Sundgren, J. E.; Rockett, A.; Motooka, T.; Greene, J. E. *Surf. Sci.* **1988**, *198*, 461.

(8) Motooka, T.; Rockett, A.; Fons, P.; Greene, J. E.; Salaneck, W. R.; Bregman, R.; Sundgren, J. E. *J. Vac. Sci. Technol.* **1988**, *6*, 3115.

By comparison to the work of Kvisle and Rytter, we assign the EELS peaks at 350, 540, 720, 1210, 1430, and 2930 cm^{-1} to the bridged Al-C stretch, the terminal Al-C stretch, the terminal CH_3 rock, the CH_3 symmetric deformation, the CH_3 asymmetric deformation, and the CH_3 asymmetric stretches, respectively, as indicated in Table I.

The data in Figures 5-7 indicate that little happens upon heating to 270 K. However, the spectra start to change at 300 K. The bridging Al-C stretching mode at 350 cm^{-1} disappears from the EELS spectrum between 300 and 400 K. Simultaneously, there is a large shift in the C_{1s} and Al_{2p} XPS peaks. Nevertheless, little desorption of decomposition products is seen.

We believe that the best explanation for these changes is that the TMAI dimers are converted to monomers between 250 and 400 K on Si(100). The absence of the bridging Al-C stretching mode is strong evidence that the dimers have broken. Further, the C_{1s} peaks have shifted from the position seen when multilayers of dimers are on the surface^{7,8} to a position close to the position of methyl groups in trimethylgallium monomers.² Thus the indications are that the TMAI dimers dissociate into monomers at around 300 K on Si(100).

Further heating causes additional changes. Methane starts to desorb. Simultaneously, the intensity of the terminal Al-C stretching mode (540 cm^{-1}) and the CH_3 stretching mode (2950 cm^{-1}) decrease in the EELS spectrum. Shoulders also appear at about 900 and 1520 cm^{-1} . Nevertheless, little change is seen in XPS.

Very similar changes were observed previously² during trimethylgallium (TMG) decomposition on Si(100). In ref 2, it was argued that the 900- and 1520- cm^{-1} modes were associated with the formation of CH_2 groups on the surface. The 900- cm^{-1} mode is in the region normally associated with CH_2 wagging modes.^{9,10} The 1520- cm^{-1} mode is at a higher frequency than normally expected for a CH_2 wagging mode in a simple hydrocarbon. However, the CH_2 wagging mode in Zeises salt for example lies at 1550 cm^{-1} .¹¹ Thus, it is not unreasonable to associate the appearance of modes at 900 and 1520 cm^{-1} with the formation of CH_2 groups on the surface. Additional arguments for these assignments are given in ref 2.

If these assignments are correct, then one can speculate about the nature of the surface intermediate produced when a monolayer of TMAI is adsorbed onto a Si(100) substrate at temperatures between 350 and 500 K. The EELS data in Figure 7 show the presence of CH_2 groups. However, there is no evidence for silicon-hydrogen stretches or growth in the region expected for silicon-carbon stretches. As a result, we suggest that at 350-500 K the CH_2 groups are still attached to the aluminum. Only minor changes in the structure of the various species has occurred.

In contrast, by 600 K we start to observe growth in the region around 800 cm^{-1} in the EELS spectrum. Our previous work shows that an 800- cm^{-1} peak is associated with the formation of Si-C bonds. Thus, it appears that some of the CH_x groups are migrating to the silicon surface at about 600 K.

Further heating causes major changes. The peaks associated with molecular TMAI are strongly attenuated in the EELS spectrum. Simultaneously, there is growth at

800 cm^{-1} , characteristic of the production of surface carbon. Further, a new peak appears at 2070 cm^{-1} , which is characteristic of a silicon-hydrogen stretch.¹² At the same time, the Al_{2p} XPS peak shifts toward that of chemisorbed aluminum, and the C_{1s} peak shifts toward that of chemisorbed carbon. Methane formation is also seen in TPD. All of these results suggest that major changes are occurring in the layer between 600 and 800 K.

Our best explanation of the 800 K EELS spectrum in Figure 7 is that the bond between the CH_x species and the aluminum atom breaks below 800 K. The process leaves carbon atoms, hydrogen atoms, aluminum atoms, and CH_x groups on the surface. The Al_{2p} XPS results are as expected if the aluminum formed islands on the surface. The C_{1s} XPS spectra are as one would expect if there were adsorbed CH_x species on the surface. There are still CH_x modes in EELS. However, there is no evidence for aluminum-carbon bonds. Thus, it appears that carbon atoms, hydrogen atoms, aluminum atoms, and CH_x groups are being produced below 800 K.

The nature of the CH_x groups cannot be unambiguously determined from the 800 K spectrum in Figure 7. However, in our previous work with TMG,² we found that a 3050- cm^{-1} peak was characteristic of the formation of CH groups on the surface. A 3050- cm^{-1} peak is seen in the 800 K spectrum in Figure 7. In the absence of other information, we speculate that CH groups are also being formed during TMAI decomposition on Si(100).

The TPD and EELS data show that the CH groups dissociate upon further heating and that the resultant hydrogen desorbs. However, XPS and EELS show that carbon remains behind on the surface to high temperatures. Calibration of our XPS results indicates that 1.3 ± 0.2 carbon atoms are deposited for every molecule of TMAI that decomposes.

If these assignments above are correct, then one can explain all of the data here via the mechanism in Figure 8. XPS and EELS show that at low-temperature TMAI dimers adsorb molecularly on the Si(100) surface. The dimers dissociate into monomers upon heating to 300-400 K. Further heating to between 400 and 600 K causes the monomers to start to decompose. Methane is seen in TPD while the formation of a CH_2 group is seen in EELS. Such results suggest that a hydrogen has been transferred from one of the methyl groups on the TMAI to another. The transfer liberates methane. The transfer process also produces a CH_2 group, as shown in Figure 8. The TPD results also show that a second hydrogen is transferred upon further heating. Simultaneously, EELS shows that CH groups form. Both observations are consistent with a hydrogen transfer from a CH_2 group to a CH_3 group, liberating methane as shown in Figure 8.

TPD does not give much information about what happens at higher temperatures. However, the XPS and EELS results show that remaining fragments decompose leaving carbon atoms, aluminum atoms, and hydrogen atoms on the surface. The hydrogen desorbs while the carbon and aluminum remain behind to high temperatures. The final Al_{2p} XPS peak is in the position expected for aluminum bound in a metallic state, while the final C_{1s} peak is in the position expected for silicon carbide. The EELS data also provide evidence for migration of CH_x groups to the support at 600 K. Thus, we conclude that TMAI decomposition follows the mechanism in Figure 8. The TMAI decomposes via a series of intramolecular hydrogen-transfer processes, yielding methane, hydrogen,

(9) Youshinobu, J.; Tsuda, H.; Onchi, M.; Nishijima, M. *J. Chem. Phys.* **1987**, *87*, 7332.

(10) Bellamy, L. J. *The Infrared Spectra Of Complex Molecules*, 3rd ed.; Chapman and Hall: London, 1985.

(11) Hiraishi, J., *Spectrochim. Acta* **1969**, *25a*, 749.

(12) Stroscio, J. A.; Bare, S. R.; Ho, W. *Surf. Sci.* **1985**, *154*, 35.

aluminum, and adsorbed carbon.

We have not included methyl radical desorption in the mechanism in Figure 8. In previous work, Squire et al.^{3,4} directed a beam of TMAI at a variety of heated substrates and used mass spectroscopy to look for desorption products. Squire et al. were not able to detect any desorption products below 650 K. However, they did observe the desorption of methyl radicals above 650 K using resonance multiphoton ionization. Unfortunately, the flux of methyl radicals could not be quantitatively determined. Squire et al. also report that they were not able to detect desorption of methane using electron impact (EI) ionization. However, the main mass fraction of methane (16 amu) is also one of the EI cracking fractions of TMAI. Thus, it is unclear whether Squire et al. could have observed methane in their experiments.

Our data show that the main carbon-containing desorption product is methane, rather than the methyl radicals reported by Squire et al. Our methods are less sensitive to methyl radicals than those used by Squire et al. However, if most of the methyl groups in the TMAI desorbed as radicals upon heating, there should not have been as much desorption of methane and hydrogen as was seen in TPD. One should also not have been able to observe the CH₂ groups, surface carbon, and surface hydrogen evident in Figure 7. Further, there should be much less residual surface carbon than is seen in Figure 6. As noted above, when we looked carefully for methyl radicals in TPD, we did detect a small peak at about 600 K in difference spectra. Thus, we cannot rule out a minor reaction pathway involving methyl radical desorption. However, we conclude that the data here are not consistent with methyl radical desorption being a major reaction pathway.

It must be pointed out, however, that Squire et al. worked under conditions much different from those used here. In particular, Squire et al. report that they get little methyl radical desorption until they build up a thick "aluminum film". We are working under conditions where the surface is nearly clean. Squire did not observe methyl radicals under such conditions. Thus, it is not surprising that methyl radical desorption is not the primary TMAI decomposition mechanism under the conditions used here.

That is unfortunate. Squire's mechanism is appealing because the methyl radical desorption pathway does not deposit carbon. As a result, if Squire's mechanism were correct, one should be able to grow carbon-free films using TMAI as a source gas for MOMBE and MOCVD. Unfortunately, under the conditions here, there is always significant carbon deposition. Notice the growth in the 800-cm⁻¹ peak in our EELS spectrum during TMAI decomposition. The 800-cm⁻¹ peak is characteristic of surface carbon which was deposited during the decomposition process. XPS also shows the presence of a significant residual carbon peak after all of the TMAI has decomposed. In fact, calibration of the XPS peaks indicates that more than a third of the carbon initially in the TMAI is left on the surface after TMAI decomposition. Thus it appears that carbon incorporation is an intrinsic part of the TMAI decomposition process on Si(100).

It is unclear what would happen on other substrates. The binding energy of a methyl group attached to a silicon atom is much larger than that of a methyl group attached to a gallium, aluminum, or arsenic atom.¹⁵ As a result, the decomposition of TMAI on a GaAs or aluminum substrate is likely to be somewhat different from that on silicon. Still, we find that the main pathway for TMAI decompo-

sition of TMAI is an intramolecular hydrogen-transfer process that is not strongly affected by the surface. As a result, the decomposition of TMAI on Al and GaAs might well follow a mechanism similar to that in Figure 8. If so, one would be left with a CH fragment on the substrate at high temperatures. The fate of the CH group is unclear. One would expect the CH fragment to be more strongly held on a silicon surface than on an aluminum or aluminum gallium arsenide surface. Hence, while the CH group decomposes upon further heating on a silicon surface, the CH group might further react to form a volatile product on an aluminum or aluminum gallium arsenide surface. Still, the mobility of a CH group is limited. Thus, the CH group's ability to react and desorb would be limited even on an Al_xGa_{1-x}As surface. As a result, if the chemistry were similar to that here, one would expect carbon incorporation to remain an intrinsic part of the TMAI decomposition process even on Al_xGa_{1-x}As.

This is not good for film growth. The fact that carbon incorporation is an intrinsic part of the TMAI decomposition process implies that *some* carbon incorporation will always occur when TMAI is used as a source gas. Admittedly, Lüth found¹⁸ that arsenic atoms will scavenge carbon. As a result, it may be possible to remove some of the carbon during film growth. However, one is not going to be able to completely overcome the problem that carbon deposition is an intrinsic part of the TMAI decomposition process. As a result TMAI would not be an appropriate source gas when one wants to produce carbon free films.

Conclusion

In summary, we conclude that TMAI dimers adsorb intact on Si(100) at temperatures below 300 K. Upon heating, the TMAI decomposes via the mechanism in Figure 8. First, the dimers decompose into monomers. Then, one of the methyl groups in the TMG reacts with a hydrogen on another methyl groups to yield methane and a CH₂ fragment. The methane desorbs while the CH₂ fragment remains bound to the gallium. Subsequently, the remaining methyl group reacts with the CH₂ fragment to yield methane and a CH fragment. Additional heating causes the CH fragment to decompose, producing hydrogen which desorbs and carbon which is incorporated into the growing film. Under our conditions, more than a third of the carbon in the TMAI is deposited onto the silicon surface. While there are ways to scavenge some of the carbon under film growth conditions, the results here suggest that TMAI would not be an appropriate source gas when one wants to produce carbon-free films.

Acknowledgment. This work was supported by the National Science Foundation under Grant DMR 86-12860. Sample preparation was done using the facilities of the University of Illinois Center for Microanalysis of Materials, which is supported as a national facility, under National Science Foundation Grant DMR 86-12860. Equipment was provided by NSF Grants CPE 83-51648 and CBT 87-04667. Helpful discussions with J. Greene and D. Lubben are greatly appreciated.

Registry No. TMAI, 75-24-1; Al, 7429-90-5; Si, 7440-21-3.

(13) Pütz, N.; Hienecke, H.; Weyers, M.; Lüth, H.; Balk, P. *J. Cryst. Growth* 1986, 74, 292.

(14) Almennigen, A.; Halvorsen, S.; Haaland, A. *Acta Chem. Scand.* 1971, 25, 1937.

(15) Coates, G. E.; Green, M. L. H.; Powell, P.; Wade, K. *Principles of Organometallic Chemistry*; Meuthen & Co.: London, 1971; p 4.